Psychoneuroendocrinology 104 (2019) 219–227

Contents lists available at ScienceDirect

Psychoneuroendocrinology

journal homepage: www.elsevier.com/locate/psyneuen

Pre-scan cortisol is differentially associated with enhanced connectivity to the cognitive control network in young adults with a history of depression

Amy T. Peters[a], Lisanne M. Jenkins[b], Jonathan P. Stange[c], Katie L. Bessette[c,d], Kristy A. Skerrett[c], Leah R. Kling[c], Robert C. Welsh[d], Mohammed R. Milad[c], Kinh L. Phan[c,e], Scott A. Langenecker[d,*]

[a] Massachusetts General Hospital, Department of Psychiatry, United States
[b] Northwestern University Feinberg School of Medicine, Department of Psychiatry and Behavioral Sciences, United States
[c] University of Illinois at Chicago, Department of Psychiatry, United States
[d] University of Utah, Department of Psychiatry, United States
[e] University of Illinois-Chicago, Department of Anatomy and Cell Biology & Graduate Program in Neuroscience, United States

ARTICLE INFO

Keywords:
Cortisol
Connectivity
Depression
Remission
fMRI

ABSTRACT

Background: We have previously demonstrated that pre-scan salivary cortisol is associated with attentuated frontal-subcortical brain activation during emotion processesing and semantic list-learning paradigms in depressed subjects. Additionally, altered functional connectivity is observed after remission of acute depression symptoms (rMDD). It is unknown whether cortisol also predicts altered functional connectivity during remission.
Methods: Participants were 47 healthy controls (HC) and 73 rMDD, 18–30 years old who provided salivary cortisol samples before and after undergoing resting-state fMRI. We tested whether salivary cortisol by diagnosis interactions were associated with seed-based resting connectivity of the default mode (DMN) and salience and emotion (SN) networks using whole-brain, cluster-level corrected ($p < .01$) regression in SPM8.
Results: Pre-scan cortisol predicted decreased (HC) and increased (rMDD) cross-network connectivity to the dorsal anterior cingulate, dorso-medial and lateral- prefrontal cortex, brain stem and cerebellum (all seeds) and precuneus (DMN seeds). By and large, pre/post-scan cortisol change predicted the same pattern of findings. In network analyses, cortisol predominantly predicted enhanced cross-network connectivity to cognitive control network regions in rMDD.
Conclusions: The association of cortisol with connections of default and salience networks to executive brain networks differs between individuals with and without a history of depression. Further investigation is needed to better understand the role of cortisol and related stress hormones as a potential primary and interactive driver of network coherence in depression.

1. Introduction

The hypothalamic-pituitary-adrenal axis (HPA-axis) is a major part of the neuroendocrine system (Bao et al., 2008; Sapolsky, 2000; Tsigos and Chrousos, 2002) that controls reactions to stress and regulates many psychophysiological responses including mood and emotions (Langenecker et al., 2012; Parker et al., 2003; Peters et al., 2016b), the immune system (Brown et al., 2004; Pariante, 2017), and energy storage and expenditure (Young et al., 1998). Major depressive disorder (MDD) is associated with HPA-axis alterations (Parker et al., 2003). Specifically, depression has been characterized by cortisol hyper-secretion (Parker et al., 2003), reduced glucocorticoid receptor mRNA expression (Hepgul et al., 2013; Pariante and Miller, 2001), and decreased glucocorticoid-induced inhibitory feedback to the HPA-axis (Rush et al., 1996).

MDD is also associated with alterations in resting-state functional magnetic resonance imaging (fMRI) networks (McEwen, 2004; Yehuda and LeDoux, 2007), including the default mode (DMN) and salience and emotion networks (SN). The DMN is involved in internally-driven mental processes, such as mind wandering, drawing on past experiences and envisioning future events (DMN; (Adler et al., 2004; Buckner and Carroll, 2007; Greicius et al., 2003; Gruberger et al., 2011). It includes mainly mid-line structures such as the posterior cingulate cortex (PCC), medial prefrontal cortex (mPFC), hippocampal formation, and precuneus, plus the angular gyrus, and lateral temporal cortices (Andrews-Hanna et al., 2014; Buckner et al., 2008). The SN is involved in

* Corresponding author at: The University of Utah, 501 Chipeta Way, Salt Lake City, UT, 84108, United States.
E-mail address: s.langenecker@hsc.utah.edu (S.A. Langenecker).

https://doi.org/10.1016/j.psyneuen.2019.03.007
Received 10 September 2018; Received in revised form 23 January 2019; Accepted 11 March 2019

detecting and filtering behaviorally relevant stimuli and coordinating integration of sensory, emotional, and cognitive information (Menon, 2011). It is primarily composed of the anterior insula, dorsal and subgenual anterior cingulate cortex (dACC; sgACC), amygdala, hypothalamus, thalamus, and striatum (Menon, 2011).

Enhanced cross-network DMN and SN connectivity has been observed to persist after remission from depression (rMDD (Jacobs et al., 2014; Lois and Wessa, 2016; Peters et al., 2016a)) and is associated with familial risk for depression (Posner et al., 2016). Specifically, increased connectivity of the DMN with the cingulate-frontal operculum system of the SN and the dorso-medial and lateral prefrontal and parietal regions of the cognitive control network (CCN) has been reported in both active and remitted depression (Drevets et al., 2008; Jacobs et al., 2014; Menon, 2011). Likewise, enhanced connectivity of the SN to lateral, parietal, and frontal regions of the CCN (Jacobs et al., 2014) and posterior midline structures of the DMN (Peters et al., 2016a) is present in rMDD.

These foci of MDD network alterations substantially overlap with the neural correlates of cortisol response to stress. For instance, enhanced cortisol response to stress induction is associated with hyperactivion of DMN regions in healthy adults, including the hippocampus, medial prefrontal cortex, and PCC. Cortisol response to stress is also associated with enhanced activation in limbic regions of the salience network (SN), including the amygdala, anterior cingulate cortex, insula, and hypothalamus, extending to the subgenual anterior cingulate (Kaiser et al., 2017; Pruessner et al., 2008; Quaedflieg et al., 2015; Vaisvaser et al., 2013; Wang et al., 2007). Moreover, we have previously illustrated that pre-scan cortisol elevations, relative to post-scan measurement and to a diurnal trend (Peters et al., 2016b; Weldon et al., 2015), are associated with attenuated frontal-subcortical activation during emotion perception (Peters et al., 2016b) and verbal list-learning in depression (Peters et al., 2018, 2016b; Weldon et al., 2015). This suggests that acute cortisol changes in anticipation of fMRI may relate broadly to regulatory brain system alterations in depression.

In line with these findings, other groups have also demonstrated that the psychological anticipation preceding fMRI procedures has been shown to evoke mild arousal of the sympathetic nervous system (Eatough et al., 2009; Lueken et al., 2012; Tessner et al., 2006), including elevated pre-scan cortisol. Elevated cortisol is present before but normalizes after the scan in both depressed (Peters et al., 2011) and healthy (Weldon et al., 2015) individuals. The extent of this arousal has also been shown to relate to neural functioning during emotion processing and decision-making tasks in both healthy (Keulers et al., 2015; Klimes-Dougan et al., 2014) and depressed subjects (Klimes-Dougan et al., 2014; Mareckova et al., 2017; Ming et al., 2017) and during remission from depression (Admon et al., 2015; Holsen et al., 2013; Ming et al., 2017). Hence, measuring and modeling whether pre-scan HPA-axis measures affect functional activation patterns differently between depressed and healthy individuals may yield valuable insights regarding adaptive and maladaptive functioning of the HPA-axis.

Beyond these initial findings using task-based fMRI, few studies have linked cortisol with altered resting-state networks. In healthy subjects, endogenous cortisol is associated with reduced amygdala-mPFC (Veer et al., 2012) and limbic (Kiem et al., 2013) connectivity, whereas cortisol awakening response predicts increased global mPFC connectivity (Wu et al., 2015). In MDD, one recent study demonstrated that morning serum cortisol was associated with reduced connectivity between the orbital-frontal cortex and cerebellum (Wang et al., 2018). To our knowledge, however, no existing studies have examined neural network associations with cortisol in rMDD, even though aberrant cross-network function may increase susceptibility to relapse (Dichter et al., 2015; Mulders et al., 2015). We were specifically interested in the effects of pre-scan cortisol seeing as fMRI scans have been shown to evoke anticipatory cortisol elevations that are present before but normalize after the scan. Thus, we assessed pre-scan cortisol-network associations in rMDD and healthy controls (HC), using resting-state fMRI.

Table 1
Demographic and clinical characteristics of rMDD and HC participants.

Variable	rMDD (n = 73) *M (SD)*	HC (n = 47) *M (SD)*	*t* or X^2	*p*
Age	22.04 (3.09)	21.61 (2.66)	0.78	.43
Female % (n)	65.7% (48)	65.9% (31)	< 0.01	.98
Education in years	15.40 (2.47)	16.21 (2.91)	1.63	.11
Verbal IQ Estimate	107.70 (9.72)	107.26 (7.44)	0.26	.79
% UIC (n)	78.1% (57)	76.6% (36)	0.04	.84
Body Mass Index[a]	25.13 (4.41)	23.98 (2.88)	−1.49	.14
Pre-scan Cortisol (μg/dl)	0.41 (0.46)	0.45 (0.71)	−0.88	.379
Post-scan Cortisol (μg/dl)[b]	0.31 (0.46)	0.39 (0.56)	0.88	.379
HDRS*	4.03 (5.16)	0.38 (.77)	4.81	< .001
Age of MDE Onset	15.53 (2.47)	–		
Current AD % (n)	17.8% (13)	–		
Current AD Plus[c]% (n)	4.1% (3)	–		

rMDD = remitted major depressive disorder; HC = Healthy Control; IQ = Intelligence Quotient; UIC = University of Illinois at Chicago; HDRS = Hamilton Depression Rating Scale; MDE = Major Depressive Episode; AD = Antidepressant medication.

* Group differences at $p < .05$.

[a] Sample n = 107; rMDD n = 64, HC n = 43).

[b] Sample n = 102; rMDD n = 65, HC n = 37.

[c] Refers to currently taking an antidepressant and additional psychiatric medications.

We hypothesized that in rMDD, pre-scan salivary cortisol would be associated with hyper-connectivity of the DMN and SN to CCN regions, and that a substantively similar pattern would be observed for pre/post-scan cortisol change.

2. Methods

2.1. Participants

rMDD (n = 73) and HC (n = 47), equivalent in terms of age, sex, and verbal IQ estimate (Table 1), were recruited for one of two NIMH-funded research studies (Research Grants: R01 MH091811, R01 MH101487) designed to assess neural networks of inhibitory control and RDoC models in mood disorders; cortisol samples were obtained for exploratory analyses. Participants were between the ages of 18–30 (M = 22.36, SD = 2.98). Trained M.A.-level clinical interviewers conducted systematic structured clinical interviews (DATA, 1997; Nurnberger et al., 1994) on all participants. rMDD previously met DSM-IV criteria for at least one historical, but not current major depressive episode, with a minimum remission duration of one month prior to enrollment. HCs had no current, past, or family history for MDD or any other psychiatric disorder. Additional exclusionary criteria included psychotherapy in the month prior to enrollment, substance abuse (past month) or dependence (past 6 months), active suicidal plan or serious attempt (past six months), serious medical illnesses or neurological illnesses, and standard contraindications to MRI (weighing > 250 pounds, pregnancy, metallic implants, pacemakers, etc.).

2.2. Procedures

Participants were enrolled at either the University of Michigan (UM) or the University of Illinois at Chicago (UIC) in accordance with respective Institutional Review Board approval. Both sites conducted an identical screening and enrollment protocol, including informed consent, diagnostic and symptom evaluation, salivary cortisol collection, and 3-Tesla neuroimaging procedures. Clinical diagnostic interviewers administered the Hamilton Depression Rating Scale (HDRS) and obtained a verbal IQ estimate (Shipley, 1982). Salivary cortisol and fMRI data were collected at a second visit. Pre-scan salivary cortisol samples were collected 10–15 min prior to fMRI, as typically there is a 10–15 min window of participant preparation related to entering the

scanner (metallic screening, participant instructions, placement, alignment). Post-scan salivary cortisol samples were collected immediately after exiting the scanner. During fMRI, participants completed an eyes-open resting-state scan acquired over 8 min, which was preceded by affect processing and working memory/executive functioning paradigms.

2.3. Saliva sample collection and cortisol assay

Saliva samples for cortisol assay were collected using Salivette Cortisol Tubes (Sarstedt AG & Co.) and stored at −80 °C until they were processed at Clinical Ligand Assay Service Satellite Laboratory at the UM School of Public Health Department or the UIC Biorepository. Immunoassay was conducted using a Siemens Centaur automated analyzer via chemiluminescent technology. The assay range was 0.012–3.000 u g/dl: no subjects were out of range. The inter- and intra-assay coefficients of variation at 0.7 μg/dl were 12.4 and 3.6%, respectively. Average pre-scan cortisol was 0.43 μg/dl. Average post-scan cortisol was 0.34 μg/dl (post-scan: $n = 102$ due to qns or values below lower limit of detection). Natural log-transformed values were computed to adjust for right-skewed cortisol values and to allow for comparison to other studies; for descriptive purposes, actual cortisol values are reported. The log-transformed and raw cortisol values were highly correlated (prescan: $r = 0.84$, $p < .001$; post-scan: $r = .81$, $p < .001$); histograms indicated the log transformed data approximated a normal distribution.

fMRI scans were administered between 8:00a.m. and 4:00 p.m., with the majority ($n = 73$, 61%) beginning and ending in the morning. Several strategies were employed to reduce the impact of the cortisol awakening response (Peters et al., 2016b). First, all participants were awake for at least one hour before the saliva collection (typical arrival time is 45 min before the scan). Second, the scanner start time was transformed into a 24-h variable and included in imaging regression analyses as a covariate of non-interest to adjust for circadian variations in cortisol across the day. Third, we ensured that rMDD and HC participants did not differ in average time of scan (for detail see Results, Salivary Cortisol).

2.4. fMRI acquisition

At UM ($n = 11$ HC, $n = 16$ rMDD), scans were collected with a 3.0 T GE Signa scanner (USA) using T2*-weighted single shot reverse spiral sequence with the following parameters: 90 ° flip, field-of-view 20, matrix size = 64 × 64, slice thickness 4 mm, 30 ms echo time, 29 slices. At UIC ($n = 36$ HC, $n = 57$ rMDD) scans were collected with a 3.0 T GE Discovery Scanner (USA) using parallel imaging with ASSET and T2* gradient-echo axial echo planar imaging (EPI) with the following parameters: 90 ° flip, field-of-view 22, matrix size = 64 × 64, slice thickness = 3 mm, 22.2 ms echo time, 44 slices. Both sites used a repetition time (TR) of 2000 ms, with 240 total TRs collected and interleaved slice acquisition. High-resolution anatomic T1 scans were obtained for spatial normalization at both sites. Motion was minimized with foam pads, by instructing participants to gaze on a visual tracking line (UIC only) and/or crosshair (UIC and UM) on the display, and by conveying the importance of holding still to participants.

2.5. fMRI preprocessing

Several steps were taken to reduce potential sources of noise and artifact as well as alignment with MNI template for uniform reporting. Slice timing was completed with SPM8 (http://www.fil.ion.ucl.ac.uk/spm/doc/, R4667) and motion detection algorithms were applied using FSL (http://fsl.fmrib.ox.ac.uk/fsl/fslwiki/, version 5.1). Coregistration of structural images to functional images was followed with spatial normalization of the coregistered T1-spgr to the MNI template. The resulting normalization matrix then was applied to the slice-time-corrected, physiologically corrected time series data. These normalized T2 time series data were spatially smoothed with a 5 mm Gaussian kernel resulting in T2 images with isotropic voxels, 2 mm on each side (Skudlarski et al., 1999). Gray matter volume was estimated following segmentation with DARTEL (VBM within SPM8) and application of a 8 mm Gaussian kernel and conversion to 2 mm isotropic voxels. All results were inspected for adverse effects of outliers.

2.6. Cross correlation analyses

Time series was de-trended and mean centered. Physiological correction was performed by regressing out the top five principal components of the masked white matter and cerebral spinal fluid signal (Behzadi et al., 2007). Motion parameters were regressed out (Jo et al., 2013) and all participants met strict motion criteria (TR to TR movement < 1.5 ° or 3 consecutive TR exceeding the same in any plane (Jacobs et al., 2014; Peters et al., 2016a)). Global signal was not regressed due to collinearity violations with gray matter signal, problematic misestimates of and introductions of anticorrelations (Fox et al., 2009), and effect on distance-micromovement relationships (Jo et al., 2013). Finally time-series were band-pass filtered over 0.01–0.10 Hz. Regions of Interest (ROIs; 2.9 mm radius, 19 voxels) were defined in MNI space. Seeds were overlaid on the average warped structural anatomy of the current sample to determine accuracy in seed location. Four bilateral seeds pairs were selected based on previous DMN and SN literature: anterior hippocampal formation (antHPF;(Schallmo et al., 2015)), PCC (Alexopoulos et al., 2012; Bluhm et al., 2011), amygdala (McCabe and Mishor, 2011; Pannekoek et al., 2013), and sgACC (Kelly et al., 2008; Margulies et al., 2007). Coordinates were: antHPF (+/−30, −12, −18), PCC (+/−5, −50, 36), amygdala (+/-23 -5 -19), and sgACC (+/−4, 21, −8). Correlation coefficients were calculated between mean time course for seed regions and all other voxels of the brain, resulting in three-dimensional correlation coefficient images (r images), transformed to Z scores using a Fisher transformation.

2.7. Data analytic approach

Clinical, demographic, and neuroendocrine measures for HC and rMDD were compared using independent samples t-tests or chi-square tests, as appropriate. A repeated measures ANOVA was used to assess change in cortisol from pre-to-post scan; residual change scores were calculated using linear regression.

For imaging analyses, z-images were used in multivariate linear regression analyses in SPM8 to assess whether the pre-scan cortisol by diagnosis interaction indicated differential cortisol-connectivity patterns in rMDD versus HC from the four bilateral seed regions (8 models). Sex, age, time of scan, HDRS, scan site, and movement parameters (roll, pitch, yaw) were covariates of no interest; main effects of cortisol that were not further qualified by a cortisol by diagnosis interaction are reported in the Supplement. All results surpassed whole-brain false-discovery rate correction of $p < .05$ by using 3dClustSim (AFNI version 16.2.19, with 1000 Monte Carlo simulations to determine the joint threshold). Our initial results were thresholded for an adjusted FWE with 4 bilateral seed analyses (2 sides by 2 networks by 2 seeds). However, given extensive results we further adjusted the threshold for simplicity in reporting (more conservative), resulting in a combined threshold for each analysis of $p < .005$ and $k > 100$. For each of eight regressions, this results in an adjusted $p < .0001$ for each regression, or a full experiment FWE of $p < .008$. Spatially averaged data for each contrast and for each participant was extracted with MARSBAR. Posthoc analyses evaluated whether pre-to-post scan cortisol change correlated with the same connectivity clusters.

We then computed tripartite resting-state network (Menon, 2011) scores (CCN, DMN, and SN) for the pre-scan cortisol x diagnostic group interaction. Network scores represent the proportion of cumulative

voxels from the interaction for each bilateral seed pair that are spatially encompassed within CCN, DMN, and SN network masks (each lateral seed network score in Supplement). The CCN mask was created by combining the dorsal attention and frontoparietal network masks from an established seven-network parcellation (Yeo et al., 2011). The SN was created by combining ventral attention and limbic networks (Yeo et al., 2011), and the original DMN parcellation was retained (Yeo et al., 2011). Subsequently, for each bilateral seed pair, network scores were compared using chi-squared tests.

3. Results

3.1. Participants

Demographic and clinical characteristics of the sample are reported in Table 1. rMDD and HC participants were equivalent in age, sex, and verbal IQ. rMDD participants had higher scores on the HDRS relative to HCs, however these remained below the clinical cutoff for MDD. Participants enrolled at the UM (n = 27) did not significantly differ in sex distribution, $\chi^2(1, 120) = .77$, $p = .512$, or HAMD score, $F(1, 119) = .29$, $p = .590$ from those enrolled at UIC. UM participants were slightly younger (M = 20.59, SD = 22.91) than UIC (M = 22.91, SD = 3.13) participants, $F(1, 119) = .12.48$, $p = .001$, verbal IQ estimate was slightly higher in UM (M = 110.89, SD = 8.78) than UIC (M = 106.53, SD = 8.67) participants, $F(1, 119) = 4.31$, $p = .040$, and UM participants were of slightly lower educational attainment (M = 14.44, SD = 1.22) than UIC (M = 16.11, SD = 2.88) participants, $F(1, 119) = 9.69$, $p = .002$. However, there were no significant site by diagnosis interactions in age, $F(2, 118) = .81$, $p = .369$, verbal IQ, $F(2, 118) = .49$, $p = .481$, education, $F(2, 118) = .71$, $p = .403$, HAMD score, $F(2, 118) = ..89$, $p = .346$, or sex, $\chi^2(1, 120) = .92$, $p = .556$, indicating that participant characteristics were adequately stratified across groups.

3.2. Salivary cortisol

Pre-scan salivary cortisol did not differ ($t = -0.88$, $p = .379$) between rMDD ($M = 0.41$, $SD = 0.46$) and HC participants ($M = 0.45$, $SD = .71$). Pre-scan cortisol did not correlate with HDRS scores ($r = .02$, $p = .830$). There was also no difference in pre-scan cortisol ($t = -0.38$, $p = .701$) between females ($M = 0.44$, $SD = 0.60$) and males ($M = 0.40$, $SD = 0.52$). Pre-scan cortisol levels were inversely correlated with time of day ($r = -0.50$, $p < .001$). Average scan start time did not differ ($t = -0.41$, $p = .678$) between rMDD ($M = 11{:}19$ am, $SD = 215$ min) and HC ($M = 11{:}01$ am, $SD = 247$ min).

Cortisol levels significantly decreased from pre-to-post scan in all subjects, $F(1,100) = 9.38$, $p = 0.003$. The rate of decrease from pre-to-post scan measurement did not differ between HC and rMDD, $F(1,100) = .006$, $p = 0.94$. Pre-scan cortisol levels were modestly correlated with the pre/post-scan residual change score ($r = 0.56$, $p < .001$).

3.3. Cortisol and DMN connectivity

3.3.1. AntHPF (Table 2)

Pre-scan cortisol was associated with increased connectivity in rMDD but decreased connectivity in HC of the antHPF to the lateral and medial PFC, inferior parietal lobule, precuneus/cuneus, and the culmen and declive of the cerebellum (Fig. 1, cyan). To illustrate, connectivity of the left antHPF to the right inferior frontal gyrus is plotted as a function of pre-scan cortisol in rMDD and HC separately (Fig. 2a). In post-hoc analyses, the pre/post cortisol change by diagnostic group interaction was significant for 8/12 clusters from the left antHPF and 7/7 clusters from the right antHPF.

3.3.2. PCC (Table 3)

Pre-scan cortisol was associated with increased connectivity in rMDD but decreased connectivity in HC of the PCC to the inferior frontal gyrus, inferior parietal cortex, parietal and occipital regions along the calcarine sulcus, and several clusters in the cerebellum (Fig. 1, blue). The pre/post cortisol change by diagnostic group interaction was significant for all clusters from both the left and right PCC.

3.4. Cortisol and SN connectivity

3.4.1. Amygdala (Table 4)

Pre-scan cortisol was associated with increased connectivity in rMDD but decreased connectivity in HC of the amygdala to the lateral and medial PFC, the inferior parietal lobule, precuneus, parahippocampal gyrus, thalamus, and caudate (Fig. 1, violet). To illustrate, connectivity of the left amygdala to the right lateral posterior thalamus is plotted as a function of pre-scan cortisol in rMDD and HC separately (Fig. 2b). The pre/post cortisol change by diagnostic group interaction was significant for 9/12 clusters from the left amygdala and 15/15 clusters from the right amygdala.

3.4.2. sgACC (Table 5)

Pre-scan cortisol was associated with increased connectivity in rMDD but decreased connectivity in HC of the sgACC to the lateral PFC, ACC, temporal gyri, uncus, precueneus, occipital-parietal junction, anterior insula, and several clusters in the cerebellum (Fig. 2, red). The pre/post cortisol change by diagnostic group interaction was significant for all clusters from the left sgACC and 11/12 clusters from the right sgACC.

3.5. Voxel-based network belongingness for foci of pre-scan cortisol by diagnostic group interactions (Fig. 3)

For the bilateral amygdala, pre-scan cortisol predicted greater connectivity in rMDD participants to the CCN relative to DMN ($\chi^2 = 51.08$, $p < .001$) and SN ($\chi^2 = 1342.02$, $p < .001$), and the DMN relative to SN ($\chi^2 = 899.76$, $p < .001$). For the bilateral sgACC; pre-scan cortisol predicted greater connectivity in rMDD participants to the CCN relative to DMN ($\chi^2 = 362.00$, $p < .001$) and SN ($\chi^2 = 929.43$, $p < .001$), and the DMN relative to SN ($\chi^2 = 153.11$, $p < .001$). For the bilateral antHPF, cortisol was associated with greater connectivity in rMDD participants to the CCN relative to DMN ($\chi^2 = 1759.59$, $p < .001$) and SN ($\chi^2 = 2622.32$, $p < .001$), and the DMN relative to SN ($\chi^2 = 147.05$, $p < .001$). For the bilateral PCC, cortisol was correlated with greater connectivity in rMDD participants of the CCN relative to the DMN ($\chi^2 = 661.61$, $p < .001$) and SN ($\chi^2 = 566.67$, $p < .001$), and the SN relative to the DMN ($\chi^2 = 460.98$, $p < .001$).

4. Discussion

Pre-scan cortisol is associated with segregation of network connectivity in HC, notably of the dorsal anterior cingulate, dorso-medial and lateral-PFC, brain stem and cerebellum (all seeds) and precuneus (DMN seeds), consistent with prior work (e.g., (Veer et al., 2012)). This study is the first to show inverted effects in rMDD where pre-scan cortisol predicts increased cross-network relationships, particularly from DMN and SN to CCN, consistent with our hypotheses. Because this occurs in a disease-specific manner, cortisol may selectively modify network function in rMDD. Alternatively, the inverted patterns may reflect compensation, or an adaptive process, which facilitates remission in rMDD.

Anatomically, the foci of connectivity associated with cortisol are broad and located throughout the brain in the medial PFC, lateral parietal lobe, visual cortex, cerebellum, medial temporal lobe, and brainstem. As cortisol exerts its influence through mineralocorticoid

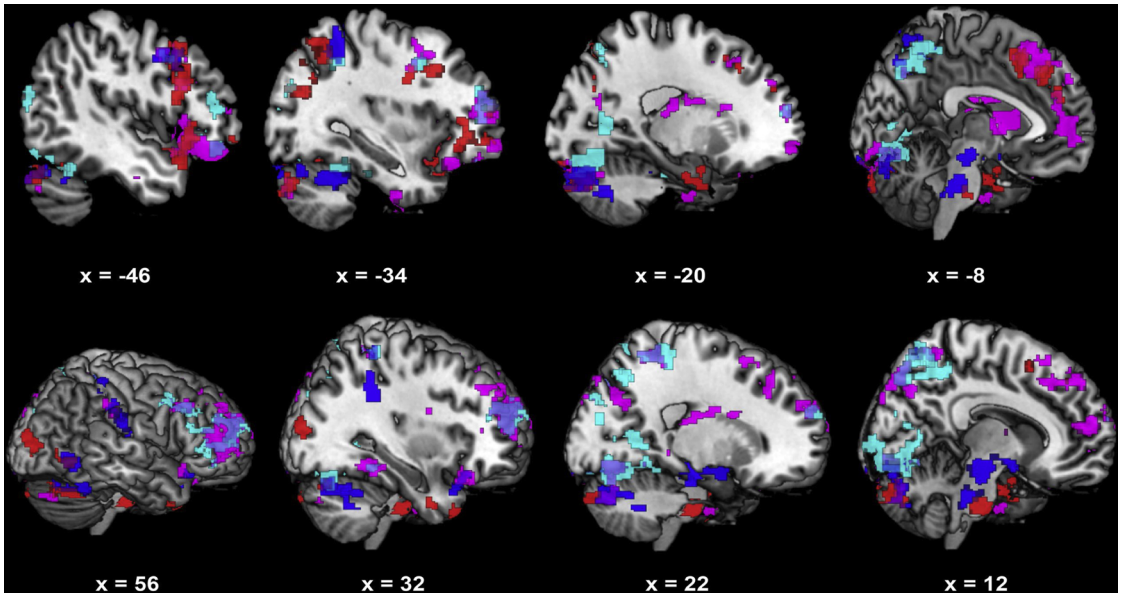

Fig. 1. Pre-scan cortisol is associated with relative hyper-connectivity of DMN and SN seed regions in rMDD compared to HC.
*Interactive Effects of Cortisol: **Blue** = Cortisol positively related to foci of connectivity from bilateral PCC seeds in rMDD but not HC; **Cyan** = Cortisol positively related to foci of connectivity from bilateral antHPF seeds in rMDD but not HC; **Red** = Cortisol positively related to foci of connectivity from bilateral sgACC seeds in rMDD but not HC; **Violet** = Cortisol positively related to foci of connectivity from bilateral amygdala seeds in rMDD but not HC. *In a multivariate analysis of covariance using extracted data for each cluster as dependent variables, all diagnosis x cortisol interactions remained significant after adjusting for BMI, $F(19, 84) = 2.52$, $p = .013$. Additionally, there were no significant main effects of BMI in relation to brain clusters reported for diagnosis x cortisol interactions $F(19, 84) = .77$, $p = .79$, nor were there any significant diagnosis x cortisol x BMI interactions $F(16, 84) = .79$, $p = .83$. (For interpretation of the references to colour in this figure legend, the reader is referred to the web version of this article).

and glucocorticoid receptors, the latter of which are more ubiquitously located in the brain (de Kloet et al., 2006; Joels and Baram, 2009), cortisol-related alterations in connectivity could be a function of cortisol binding to glucocorticoid receptors in these areas. For instance, both DMN and SN seeds show robust connectivity to the medial PFC, where concentrations of glucocorticoid receptors are particularly high (Diorio et al., 1993). Molecular probes of glucocorticoid receptors, such as in positron emission tomography, should more formally test this hypothesis.

It is provocative that cortisol was associated with *opposing* effects on cross-network connectivity to the CNN in rMDD versus HC. Additionally, for convergence, the majority of the effects were retained when using pre/post scan change in cortisol as the regresssor. It has been proposed that segregation of networks (higher within-network coherence) may optimize the specialization of brain systems whose regions are distributed anatomically, but are in the service of similar functions (Chan et al., 2014). As cortisol was related to over-integration from the DMN and SN to the CCN in rMDD, speculatively, enhanced connectivity of networks to the CCN may challenge the functional specialization and efficiency of each network. Through this lens, higher cross-talk of the cognitive control with other networks could represent regulation (enhancement for remission) or interference (decreased

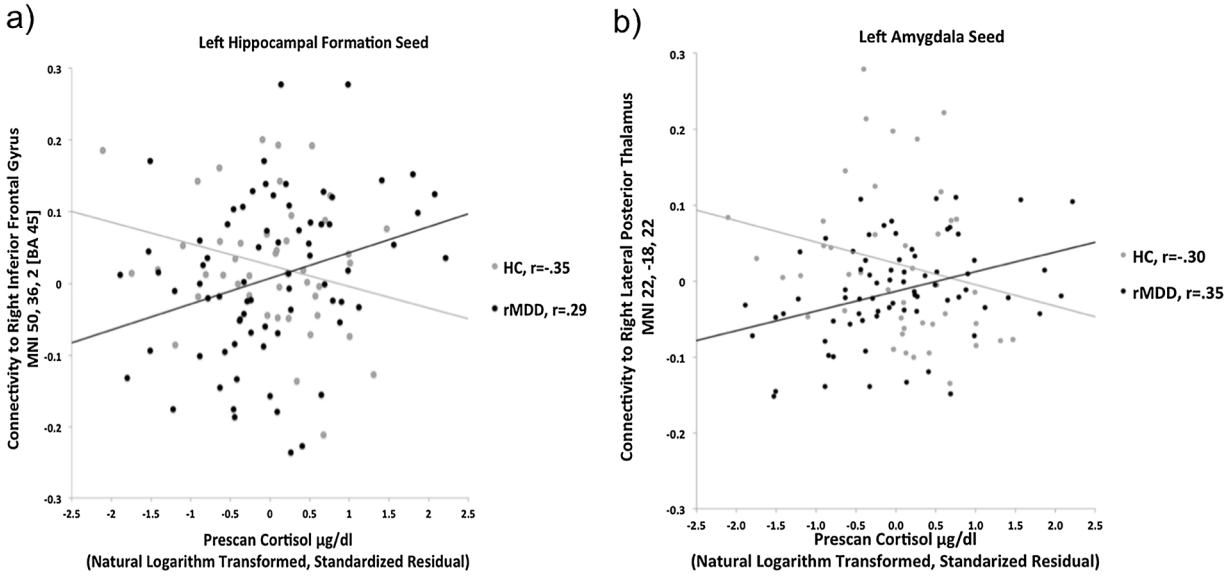

Fig. 2. a) Differential association of pre-scan cortisol with connectivity of the left antHPF seed in rMDD vs. HC; b) Differential association of pre-scan cortisol with connectivity of the left amygdala seed in rMDD vs. HC.

Table 2
Foci of connectivity in pre-scan cortisol regression from bilateral anterior hippocampal formation seed.

	Left antHPF Seed						Right antHPF Seed					
		MNI coordinates						MNI coordinates				
Contrast/Lobe	BA	x	y	z	Z	k	BA	x	y	z	Z	k
Cortisol by Diagnosis Interaction												
Positive Association in rMDD												
Frontal												
Superior Frontal	10	−24	56	14	3.63	103[a]	10	24	58	22	4.06	540
Precentral	9	−42	8	40	4.08	165	–	–	–	–	–	–
Middle Frontal	6/9	−38	−80	24	3.71	179	9/10	−28	54	16	3.45	512
	9/46	48	22	24	3.13	133[a]	9/46	50	24	34	3.91	255
Inferior Frontal	45/47	50	36	2	3.57	207	45/47	−52	28	0	3.45	127
Parietal												
Inferior Parietal Lobule	40	−60	−32	30	3.25	110[a]	–	–	–	–	–	–
Precuneus	7	−8	−54	54	4.57	1597	7	−10	−58	54	3.99	220
	–	–	–	–	–	–	7	10	−58	58	3.56	189 [a]
Temporal												
Inferior Temporal	20	−58	−46	−6	3.57	315	–	–	–	–	–	–
Occipital												
Cuneus	18	14	−80	22	3.37	152	–	–	–	–	–	–
Lingual Gyrus	18	8	−88	−10	4.68	2288	–	–	–	–	–	–
Subcortical												
Cerebellum, Culmen		−30	−44	−24	4.05	342		–	–	–	–	–
Cerebellum, Declive		–	–	–	–	–		−46	−76	−16	3.23	109

[a] Attenuated to trend effects and no longer reached the statistically significant threshold in sensitivity analyses excluding UM participants.

Table 3
Foci of connectivity in pre-scan cortisol regression from bilateral posterior cingulate cortex seed.

	Left PCC Seed						Right PCC Seed					
		MNI coordinates						MNI coordinates				
Contrast/Lobe	BA	x	y	z	Z	k	BA	x	y	z	Z	k
Cortisol by Diagnosis Interaction												
Positive Association in rMDD												
Frontal												
Inferior Frontal	–	–	–	–	–	–	44	−56	10	18	3.8	362
Parietal												
Inferior Parietal Lobule	40	−60	−34	34	3.23	128	40	−62	−32	32	3.39	236
							40	68	−22	24	3.48	251
	–	–	–	–	–	–	40	44	−36	56	3.43	141 [a]
Precuneus	7	−10	−46	54	3.43	253	7	−10	−46	54	3.31	102
Temporal												
Superior Temporal	–	–	–	–	–	–	38	36	16	−28	4.17	169
Occipital												
Middle Occipital	37	58	−62	−4	3.64	223	–	–	–	–	–	–
Subcortical												
Cerebellum, Tuber		−44	−74	−26	4.02	1113		–	–	–	–	–
Cerebellum, Culmen		12	−20	−18	4.54	554		–	–	–	–	–
Cerebellum, Anterior Cerebellar		42	−52	−30	4.5	275		−34	−54	−28	4.25	334
								44	−52	−30	4.75	1633
Cerebellum, Cerebellar Tonsil		–	–	–	–	–		−34	−48	50	4.28	300

[a] Attenuated to trend effects and no longer reached the statistically significant threshold in sensitivity analyses excluding UM participants.

efficiency as a disease marker) and may pose risk for depression or represent compensatory mechanisms.

There are some patterns of rMDD connectivity according to seed region that warrant additional discussion. First, PCC connectivity was somewhat attenuated to the CCN and enhanced to the SN, compared to other seeds, particularly the antHPF. Perhaps this pattern reflects that cortisol is differentially relevant to ventral and dorsal sub-components of the DMN (Bessette et al., 2018; Buckner et al., 2008). The antHPF seeds may more closely mirror results from the amygdala and sgACC because of density in MR and GR receptors, which are more sparsely distributed in the PCC (Sapolsky, 2000; Tsigos and Chrousos, 2002). Additionally, the PCC and antHPF showed largely bilateral effects, especially to the mid-brain and visual cortex, whereas connectivity of the sgACC and amygdala were somewhat lateralized, more so to the left PFC. Interestingly, the left PFC is a common target for antidepressant transcranial magnetic stimulation (Schutter, 2008) and its efficacy is associated with left dorsolateral PFC and sgACC anti-correlation (Fox et al., 2012). This gives rise to the possibility that anti-depressant effects of non-invasive stimulation could partly work through modulating disrupted neuroendocrine systems.

One limitation of this study is the cortisol awakening response represents a challenge in neuroendocrine assessment (Stalder et al., 2016) and we cannot rule out the influence of time of day on inter-subject variability, given a lack of a true baseline for comparison. Future studies should use fixed circadian time points for cortisol assessment and scanning, or alternatively, utilize the daily slope in cortisol across multiple measurements. Additionally, HPA-axis time scale is on the order of minutes; 10–30 min transpire between CRH surges and the

Table 4
Foci of connectivity in pre-scan cortisol regression from bilateral amygdala seed.

	Left Amygdala Seed						Right Amygdala Seed					
		MNI coordinates						MNI coordinates				
Contrast/Lobe	BA	x	y	z	Z	k	BA	x	y	z	Z	k
Cortisol by Diagnosis Interaction												
Positive Association in rMDD												
Frontal												
Superior Frontal	10	−28	54	14	4.29	318	9/10	14	62	26	3.39	489
Precentral	–	–	–	–	–	–	9/10	−42	8	42	4.45	356
	–	–	–	–	–	–	9/10	−50	24	26	3.37	103[a]
Middle Frontal	10	−38	58	−8	3.74	108	10	−34	48	14	4.61	507
	10	38	54	12	3.86	958	9/10	44	24	38	3.33	140
Medial Frontal	–	–	–	–	–	–	8	−6	32	48	4.40	1254
Inferior	–	–	–	–	–	–	47	44	18	−16	3.91	230
Parietal												
Inferior Parietal Lobule	40	60	−28	34	3.65	195[a]	–	–	–	–	–	–
Precuneus	–	–	–	–	–	–	7	14	−52	58	3.54	167
Temporal												
Parahippocampal Gyrus	30	28	−46	−12	3.42	181	30/36	−48	34	−14	4.98	1732
Inferior Temporal	–	–	–	–	–	–	20	−56	−8	−28	3.64	176
Uncus	36	−28	−8	−40	3.60	111	–	–	–	–	–	–
Occipital												
Precuneus	11	−12	−66	−26	3.15	138	–	–	–	–	–	–
Cuneus	17/18/19	6	−78	46	4.33	661	17	−10	−82	−18	3.39	164
Subcortical												
Thalamus, Lateral Posterior Nucleus/Pulvinar		22	−18	22	3.99	222		−16	−20	20	3.52	150
Caudate		–	–	–	–	–		−12	10	10	3.75	297
Cerebellum, Declive		0	−80	−10	3.23	272		–	–	–	–	–
		20	−76	−12	3.52	142[a]		–	–	–	–	–
Cerebellum, Tuber		−44	−82	−28	4.00	100		–	–	–	–	–
Cerebellum, Pyramis		–	–	–	–	–		22	−78	−34	3.88	443
Cerebellum, Inferior Semi Lunar Lobule								−26	−82	−38	4.01	305

[a] Attenuated to trend effects and no longer reached the statistically significant threshold in sensitivity analyses excluding UM participants.

Table 5
Foci of connectivity in pre-scan cortisol regression from bilateral subgenual anterior cingulate cortex seed.

	Left SgACC Seed						Right SgACC Seed					
		MNI coordinates						MNI coordinates				
Contrast/Lobe	BA	x	y	z	Z	k	BA	x	y	z	Z	k
Cortisol by Diagnosis Interaction												
Positive Association in rMDD												
Frontal												
Anterior Cingulate	32	−12	26	42	3.61	495	–	–	–	–	–	–
Middle Frontal	6/8/9	−42	20	24	3.97	631	6/8/9	−4	34	40	3.90	300[a]
Inferior Frontal	47	−42	28	−6	3.60	478	47	−44	24	−4	3.66	334
							45	−38	34	6	3.50	119
Parietal												
Precuneus	7	−26	−74	58	3.42	569	–	–	–	–	–	–
Temporal												
Superior Temporal	38	38	14	−36	3.66	172	39	−56	−56	26	3.47	150[a]
Fusiform Gyrus	–	–	–	–	–	–	37	54	−60	−8	3.66	121
Uncus	34	−20	0	−22	3.51	114	–	–	–	–	–	–
Occipital												
Middle Occipital	19	−58	−62	0	3.44	277[a]	19	−58	−62	−2	3.55	218
	19	36	−90	10	3.40	175	–	–	–	–	–	–
Precuneus	–	–	–	–	–	–	31	−30	−74	24	3.58	181
	–	–	–	–	–	–	31	54	−60	−32	3.71	203[a]
Subcortical												
Anterior Insula							13	−46	14	16	3.72	319[a]
Cerebellum, Tuber		−44	−74	−26	4.01	476		–	–	–	–	–
Cerebellum, Pyramis	–	–	–	–	–	–		−16	−82	−30	4.25	1055
Cerebellum, Inferior Semi Lunar Lobule	–	–	–	–	–	–		12	−78	−36	3.80	302

[a] Attenuated to trend effects and no longer reached the statistically significant threshold in sensitivity analyses excluding UM participants.

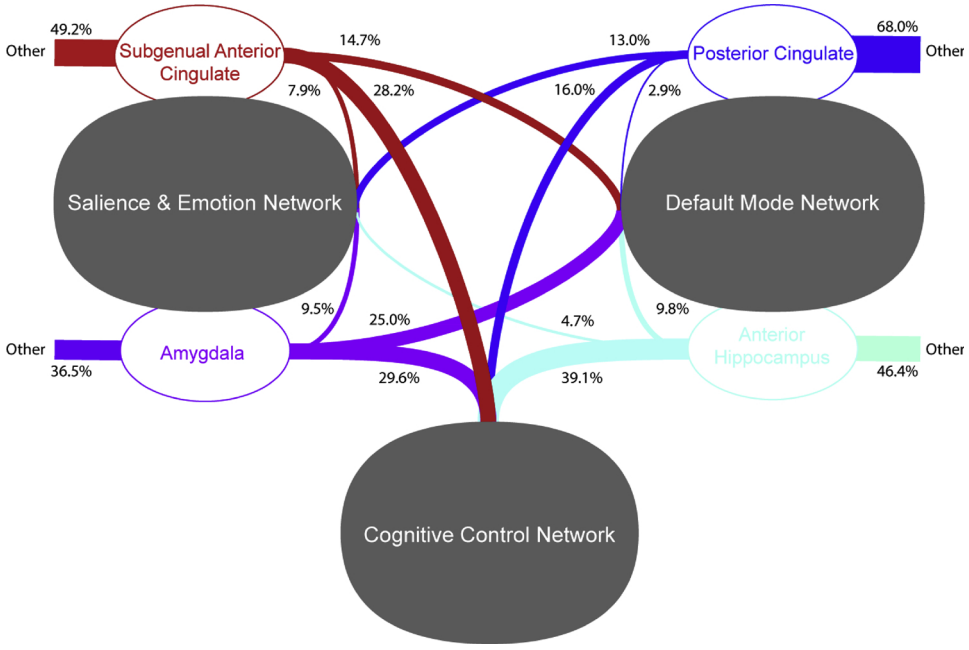

Fig. 3. Voxel-Based Network Belongingness for Foci of Pre-scan Cortisol by Diagnostic Group Interactions in Seed-Based Connectivity Analyses.

cortisol response. Accordingly, cortisol may relate to more stable network relationships than short-term temporal modulations. Further, participants were recruited from two different sites and it was not possible to fully isolate the introduction of potentional effects or variability due to the scanners and site-specific settings. Third, basal cortisol levels and diurnal rhythm were not assessed in this exploratory study, so the exact meaning of the cortisol associations remains for future, more tightly controlled experiments. Specifically, inclusion of true pre/post stress tests and perceived stress measures will be essential. Last, resting state scans were preceded by cognitive and emotional tasks and we cannot rule out possible carryover effects related to the demands of these tasks on brain connectivity or cortisol.

Strengths of this study include a well-powered sample, conservative analytic threshold, co-measurement of salivary cortisol and neural networks, and a young sample, early in the course of illness, that is not confounded by the burden of chronicity and morbidity. This study is the first to demonstrate that the association of cortisol with cross-network connectivity differs in rMDD versus HC. Coupled with prior task-based work (Peters et al., 2016b; Weldon et al., 2015), resting emotional and introspective network connectivity to the CCN may occur at the expense of external task performance, by failing to disengage internal ones. Thus, cortisol may facilitate CCN regulation in rMDD, possibly reflecting compensatory mechanisms of resilience or trait markers of depression. Moreover, that pre-scan cortisol reflects prominent between group differences in connectivity underscores the methodological importance of including cortisol measurement in fMRI studies.

Conflict of interests

None of the authors have conflicts of interest to disclose.

Appendix A. Supplementary data

Supplementary material related to this article can be found, in the online version, at doi:https://doi.org/10.1016/j.psyneuen.2019.03.007.

References

Adler, C.M., Holland, S.K., Schmithorst, V., Tuchfarber, M.J., Strakowski, S.M., 2004. Changes in neuronal activation in patients with bipolar disorder during performance of a working memory task. Bipolar Disord. 6, 540–549.
Admon, R., Holsen, L.M., Aizley, H., Remington, A., Whitfield-Gabrieli, S., Goldstein, J.M., Pizzagalli, D.A., 2015. Striatal hypersensitivity during stress in remitted individuals with recurrent depression. Biol. Psychiatry 78, 67–76.
Alexopoulos, G.S., Hoptman, M.J., Kanellopoulos, D., Murphy, C.F., Lim, K.O., Gunning, F.M., 2012. Functional connectivity in the cognitive control network and the default mode network in late-life depression. J. Affect. Disord. 139, 56–65.
Andrews-Hanna, J.R., Smallwood, J., Spreng, R.N., 2014. The default network and self-generated thought: component processes, dynamic control, and clinical relevance. Ann. N. Y. Acad. Sci. 1316, 29–52.
Bao, A.M., Meynen, G., Swaab, D.F., 2008. The stress system in depression and neurodegeneration: focus on the human hypothalamus. Brain Res. Rev. 57, 531–553.
Behzadi, Y., Restom, K., Liau, J., Liu, T.T., 2007. A component based noise correction method (CompCor) for BOLD and perfusion based fMRI. Neuroimage 37, 90–101.
Bessette, K.L., Jenkins, L.M., Skerrett, K.A., Gowins, J.R., DelDonno, S.R., Zubieta, J.K., McInnis, M.G., Jacobs, R.H., Ajilore, O., Langenecker, S.A., 2018. Reliability, convergent validity and time invariance of default mode network deviations in early adult major depressive disorder. Front. Psychiatry 9, 244.
Bluhm, R.L., Clark, C.R., McFarlane, A.C., Moores, K.A., Shaw, M.E., Lanius, R.A., 2011. Default network connectivity during a working memory task. Hum. Brain Mapp. 32, 1029–1035.
Brown, E.S., Varghese, F.P., McEwen, B.S., 2004. Association of depression with medical illness: does cortisol play a role? Biol. Psychiatry 55, 1–9.
Buckner, R.L., Carroll, D.C., 2007. Self-projection and the brain. Trends Cogn. Sci. 11, 49–57.
Buckner, R.L., Andrews-Hanna, J.R., Schacter, D.L., 2008. The brain's default network: anatomy, function, and relevance to disease. Ann. N. Y. Acad. Sci. 1124, 1–38.
Chan, M.Y., Park, D.C., Savalia, N.K., Petersen, S.E., Wig, G.S., 2014. Decreased segregation of brain systems across the healthy adult lifespan. Proc. Natl. Acad. Sci. U. S. A. 111, E4997–5006.
DATA, D., 1997. Structured Clinical Interview for DSM-IV Axis I Disorders. American Psychiatric Press, Washington.
de Kloet, C.S., Vermetten, E., Geuze, E., Kavelaars, A., Heijnen, C.J., Westenberg, H.G., 2006. Assessment of HPA-axis function in posttraumatic stress disorder: pharmacological and non-pharmacological challenge tests, a review. J. Psychiatr. Res. 40, 550–567.
Dichter, G.S., Gibbs, D., Smoski, M.J., 2015. A systematic review of relations between resting-state functional-MRI and treatment response in major depressive disorder. J. Affect. Disord. 172, 8–17.
Diorio, D., Viau, V., Meaney, M.J., 1993. The role of the medial prefrontal cortex (cingulate gyrus) in the regulation of hypothalamic-pituitary-adrenal responses to stress. J. Neurosci. 13, 3839–3847.
Drevets, W.C., Price, J.L., Furey, M.L., 2008. Brain structural and functional abnormalities in mood disorders: implications for neurocircuitry models of depression. Brain Struct. Funct. 213, 93–118.
Eatough, E.M., Shirtcliff, E.A., Hanson, J.L., Pollak, S.D., 2009. Hormonal reactivity to MRI scanning in adolescents. Psychoneuroendocrinology 34, 1242–1246.
Fox, M.D., Zhang, D., Snyder, A.Z., Raichle, M.E., 2009. The global signal and observed anticorrelated resting state brain networks. J. Neurophysiol. 101, 3270–3283.
Fox, M.D., Buckner, R.L., White, M.P., Greicius, M.D., Pascual-Leone, A., 2012. Efficacy of transcranial magnetic stimulation targets for depression is related to intrinsic

functional connectivity with the subgenual cingulate. Biol. Psychiatry 72, 595–603.
Greicius, M.D., Krasnow, B., Reiss, A.L., Menon, V., 2003. Functional connectivity in the resting brain: a network analysis of the default mode hypothesis. Proc. Natl. Acad. Sci. U. S. A. 100, 253–258.
Gruberger, M., Ben-Simon, E., Levkovitz, Y., Zangen, A., Hendler, T., 2011. Towards a neuroscience of mind-wandering. Front. Hum. Neurosci. 5, 56.
Hepgul, N., Cattaneo, A., Zunszain, P.A., Pariante, C.M., 2013. Depression pathogenesis and treatment: what can we learn from blood mRNA expression? BMC Med. 11, 28.
Holsen, L.M., Lancaster, K., Klibanski, A., Whitfield-Gabrieli, S., Cherkerzian, S., Buka, S., Goldstein, J.M., 2013. HPA-axis hormone modulation of stress response circuitry activity in women with remitted major depression. Neuroscience 250, 733–742.
Jacobs, R.H., Jenkins, L.M., Gabriel, L.B., Barba, A., Ryan, K.A., Weisenbach, S.L., Verges, A., Baker, A.M., Peters, A.T., Crane, N.A., Gotlib, I.H., Zubieta, J.K., Phan, K.L., Langenecker, S.A., Welsh, R.C., 2014. Increased coupling of intrinsic networks in remitted depressed youth predicts rumination and cognitive control. PLoS One 9, e104366.
Jo, H.J., Gotts, S.J., Reynolds, R.C., Bandettini, P.A., Martin, A., Cox, R.W., Saad, Z.S., 2013. Effective preprocessing procedures virtually eliminate distance-dependent motion artifacts in resting state FMRI. J. Appl. Math. 2013.
Joels, M., Baram, T.Z., 2009. The neuro-symphony of stress. Nat. Rev. Neurosci. 10, 459–466.
Kaiser, R.H., Clegg, R., Goer, F., Pechtel, P., Beltzer, M., Vitaliano, G., Olson, D.P., Teicher, M.H., Pizzagalli, D.A., 2017. Childhood stress, grown-up brain networks: corticolimbic correlates of threat-related early life stress and adult stress response. Psychol. Med. 1–13.
Kelly, A.C., Di Martino, A., Uddin, L.Q., Shehzad, Z., Gee, D.G., Reiss, P.T., Margulies, D.S., Castellanos, F.X., Milham, M.P., 2008. Development of anterior cingulate functional connectivity from late childhood to early adulthood. Cereb. Cortex 19, 640–657.
Keulers, E.H., Stiers, P., Nicolson, N.A., Jolles, J., 2015. The association between cortisol and the BOLD response in male adolescents undergoing fMRI. Brain Res. 1598, 1–11.
Kiem, S.A., Andrade, K.C., Spoormaker, V.I., Holsboer, F., Czisch, M., Samann, P.G., 2013. Resting state functional MRI connectivity predicts hypothalamus-pituitary-axis status in healthy males. Psychoneuroendocrinology 38, 1338–1348.
Klimes-Dougan, B., Eberly, L.E., Westlund Schreiner, M., Kurkiewicz, P., Houri, A., Schlesinger, A., Thomas, K.M., Mueller, B.A., Lim, K.O., Cullen, K.R., 2014. Multilevel assessment of the neurobiological threat system in depressed adolescents: interplay between the limbic system and hypothalamic-pituitary-adrenal axis. Dev. Psychopathol. 26, 1321–1335.
Langenecker, S.A., Weisenbach, S.L., Giordani, B., Briceno, E.M., Guidotti Breting, L.M., Schallmo, M.P., Leon, H.M., Noll, D.C., Zubieta, J.K., Schteingart, D.E., Starkman, M.N., 2012. Impact of chronic hypercortisolemia on affective processing. Neuropharmacology 62, 217–225.
Lois, G., Wessa, M., 2016. Differential association of default mode network connectivity and rumination in healthy individuals and remitted MDD patients. Soc. Cogn. Affect. Neurosci. 11, 1792–1801.
Lueken, U., Muehlhan, M., Evens, R., Wittchen, H.U., Kirschbaum, C., 2012. Within and between session changes in subjective and neuroendocrine stress parameters during magnetic resonance imaging: a controlled scanner training study. Psychoneuroendocrinology 37, 1299–1308.
Mareckova, K., Holsen, L., Admon, R., Whitfield-Gabrieli, S., Seidman, L.J., Buka, S.L., Klibanski, A., Goldstein, J.M., 2017. Neural - hormonal responses to negative affective stimuli: impact of dysphoric mood and sex. J. Affect. Disord. 222, 88–97.
Margulies, D.S., Kelly, A.C., Uddin, L.Q., Biswal, B.B., Castellanos, F.X., Milham, M.P., 2007. Mapping the functional connectivity of anterior cingulate cortex. Neuroimage 37, 579–588.
McCabe, C., Mishor, Z., 2011. Antidepressant medications reduce subcortical–cortical resting-state functional connectivity in healthy volunteers. Neuroimage 57, 1317–1323.
McEwen, B.S., 2004. Protection and damage from acute and chronic stress: allostasis and allostatic overload and relevance to the pathophysiology of psychiatric disorders. Ann. N. Y. Acad. Sci. 1032, 1–7.
Menon, V., 2011. Large-scale brain networks and psychopathology: a unifying triple network model. Trends Cogn. Sci. 15, 483–506.
Ming, Q., Zhong, X., Zhang, X., Pu, W., Dong, D., Jiang, Y., Gao, Y., Wang, X., Detre, J.A., Yao, S., Rao, H., 2017. State-independent and dependent neural responses to psychosocial stress in current and remitted depression. Am. J. Psychiatry 174, 971–979.
Mulders, P.C., van Eijndhoven, P.F., Schene, A.H., Beckmann, C.F., Tendolkar, I., 2015. Resting-state functional connectivity in major depressive disorder: a review. Neurosci. Biobehav. Rev. 56, 330–344.
Nurnberger, J.I., Blehar, M.C., Kaufmann, C.A., York-Cooler, C., Simpson, S.G., Harkavy-Friedman, J., Severe, J.B., Malaspina, D., Reich, T., 1994. Diagnostic interview for genetic studies: rationale, unique features, and training. Arch. Gen. Psychiatry 51, 849–859.
Pannekoek, J.N., Veer, I.M., van Tol, M.-J., van der Werff, S.J., Demenescu, L.R., Aleman, A., Veltman, D.J., Zitman, F.G., Rombouts, S.A., van der Wee, N.J., 2013. Aberrant limbic and salience network resting-state functional connectivity in panic disorder without comorbidity. J. Affect. Disord. 145, 29–35.
Pariante, C.M., 2017. Why are depressed patients inflamed? A reflection on 20 years of research on depression, glucocorticoid resistance and inflammation. Eur. Neuropsychopharmacol. 27, 554–559.
Pariante, C.M., Miller, A.H., 2001. Glucocorticoid receptors in major depression: relevance to pathophysiology and treatment. Biol. Psychiatry 49, 391–404.
Parker, K.J., Schatzberg, A.F., Lyons, D.M., 2003. Neuroendocrine aspects of hypercortisolism in major depression. Horm. Behav. 43, 60–66.
Peters, S., Cleare, A.J., Papadopoulos, A., Fu, C.H., 2011. Cortisol responses to serial MRI scans in healthy adults and in depression. Psychoneuroendocrinology 36, 737–741.
Peters, A.T., Burkhouse, K., Feldhaus, C.C., Langenecker, S.A., Jacobs, R.H., 2016a. Aberrant resting-state functional connectivity in limbic and cognitive control networks relates to depressive rumination and mindfulness: a pilot study among adolescents with a history of depression. J. Affect. Disord. 200, 178–181.
Peters, A.T., Van Meter, A., Pruitt, P.J., Briceno, E.M., Ryan, K.A., Hagan, M., Weldon, A.L., Kassel, M.T., Vederman, A., Zubieta, J.K., McInnis, M., Weisenbach, S.L., Langenecker, S.A., 2016b. Acute cortisol reactivity attenuates engagement of frontoparietal and striatal regions during emotion processing in negative mood disorders. Psychoneuroendocrinology 73, 67–78.
Peters, A.T., Smith, R.A., Kassel, M.T., Hagan, M., Maki, P., Van Meter, A., Briceno, E.M., Ryan, K.A., Weldon, A.L., Weisenbach, S.L., Starkman, M.N., Langenecker, S.A., 2018. A pilot investigation of differential neuroendocrine associations with frontolimbic activation during semantically-cued list learning in mood disorders. J. Affect. Disord. 239, 180–191.
Posner, J., Cha, J., Wang, Z., Talati, A., Warner, V., Gerber, A., Peterson, B.S., Weissman, M., 2016. Increased default mode network connectivity in individuals at high familial risk for depression. Neuropsychopharmacology 41, 1759–1767.
Pruessner, J.C., Dedovic, K., Khalili-Mahani, N., Engert, V., Pruessner, M., Buss, C., Renwick, R., Dagher, A., Meaney, M.J., Lupien, S., 2008. Deactivation of the limbic system during acute psychosocial stress: evidence from positron emission tomography and functional magnetic resonance imaging studies. Biol. Psychiatry 63, 234–240.
Quaedflieg, C.W., van de Ven, V., Meyer, T., Siep, N., Merckelbach, H., Smeets, T., 2015. Temporal dynamics of stress-induced alternations of intrinsic amygdala connectivity and neuroendocrine levels. PLoS One 10, e0124141.
Rush, A.J., Giles, D.E., Schlesser, M.A., Orsulak, P.J., Parker Jr., C.R., Weissenburger, J.E., Crowley, G.T., Khatami, M., Vasavada, N., 1996. The dexamethasone suppression test in patients with mood disorders. J. Clin. Psychiatry 57, 470–484.
Sapolsky, R., 2000. Glucocorticoids and hippocampal atrophy in neuropsychiatric disorders. Arch. Gen. Psychiatry 57, 925–935.
Schallmo, M.-P., Kassel, M.T., Weisenbach, S.L., Walker, S.J., Guidotti-Breting, L.M., Rao, J.A., Hazlett, K.E., Considine, C.M., Sethi, G., Vats, N., 2015. A new semantic list learning task to probe functioning of the Papez circuit. J. Clin. Exp. Neuropsychol. 37, 816–833.
Schutter, D.J.L.G., 2008. Antidepressant efficacy of high-frequency transcranial magnetic stimulation over the left dorsolateral prefrontal cortex in double-blind sham-controlled designs: a meta-analysis. Psychol. Med. 39, 65–75.
Shipley, W.C., 1982. Shipley Institute of Living Scale: For Measuring Intellectual Impairment. Western Psychological Services.
Skudlarski, P., Constable, R.T., Gore, J.C., 1999. ROC analysis of statistical methods used in functional MRI: individual subjects. Neuroimage 9, 311–329.
Stalder, T., Kirschbaum, C., Kudielka, B.M., Adam, E.K., Pruessner, J.C., Wust, S., Dockray, S., Smyth, N., Evans, P., Hellhammer, D.H., Miller, R., Wetherell, M.A., Lupien, S.J., Clow, A., 2016. Assessment of the cortisol awakening response: expert consensus guidelines. Psychoneuroendocrinology 63, 414–432.
Tessner, K.D., Walker, E.F., Hochman, K., Hamann, S., 2006. Cortisol responses of healthy volunteers undergoing magnetic resonance imaging. Hum. Brain Mapp. 27, 889–895.
Tsigos, C., Chrousos, G.P., 2002. Hypothalamic-pituitary-adrenal axis, neuroendocrine factors and stress. J. Psychosom. Res. 53, 865–871.
Vaisvaser, S., Lin, T., Admon, R., Podlipsky, I., Greenman, Y., Stern, N., Fruchter, E., Wald, I., Pine, D.S., Tarrasch, R., Bar-Haim, Y., Hendler, T., 2013. Neural traces of stress: cortisol related sustained enhancement of amygdala-hippocampal functional connectivity. Front. Hum. Neurosci. 7, 313.
Veer, I.M., Oei, N.Y., Spinhoven, P., van Buchem, M.A., Elzinga, B.M., Rombouts, S.A., 2012. Endogenous cortisol is associated with functional connectivity between the amygdala and medial prefrontal cortex. Psychoneuroendocrinology 37, 1039–1047.
Wang, J., Korczykowski, M., Rao, H., Fan, Y., Pluta, J., Gur, R.C., McEwen, B.S., Detre, J.A., 2007. Gender difference in neural response to psychological stress. Soc. Cogn. Affect. Neurosci. 2, 227–239.
Wang, Y., Chen, G., Zhong, S., Jia, Y., Xia, L., Lai, S., Zhao, L., Huang, L., Liu, T., 2018. Association between resting-state brain functional connectivity and cortisol levels in unmedicated major depressive disorder. J. Psychiatr. Res. 105, 55–62.
Weldon, A.L., Hagan, M., Van Meter, A., Jacobs, R.H., Kassel, M.T., Hazlett, K.E., Haase, B.D., Vederman, A.C., Avery, E., Briceno, E.M., Welsh, R.C., Zubieta, J.K., Weisenbach, S.L., Langenecker, S.A., 2015. Stress response to the functional magnetic resonance imaging environment in healthy adults relates to the degree of limbic reactivity during emotion processing. Neuropsychobiology 71, 85–96.
Wu, J., Zhang, S., Li, W., Qin, S., He, Y., Yang, Z., Buchanan, T.W., Liu, C., Zhang, K., 2015. Cortisol awakening response predicts intrinsic functional connectivity of the medial prefrontal cortex in the afternoon of the same day. Neuroimage 122, 158–165.
Yehuda, R., LeDoux, J., 2007. Response variation following trauma: a translational neuroscience approach to understanding PTSD. Neuron 56, 19–32.
Yeo, B.T., Krienen, F.M., Sepulcre, J., Sabuncu, M.R., Lashkari, D., Hollinshead, M., Roffman, J.L., Smoller, J.W., Zollei, L., Polimeni, J.R., Fischl, B., Liu, H., Buckner, R.L., 2011. The organization of the human cerebral cortex estimated by intrinsic functional connectivity. J. Neurophysiol. 106, 1125–1165.
Young, E., Lopez, J.F., Weinberg, V.M., Watson, S.J., Akil, H., 1998. The role of mineralocorticoid receptors in Hypothalamic-pituitary-adrenal axis regulation in humans. J. Clin. Endocrinol. Metab. 83, 3339–3345.